Production of relativistic antihydrogen atoms by pair production with positron capture

Charles T. Munger and Stanley J. Brodsky
Stanford Linear Accelerator Center, Stanford University, Stanford, California 94309

Ivan Schmidt
Universidad Federico Santa María, Casilla 110-V, Valparaíso, Chile

(Received 9 June 1993)

A beam of relativistic antihydrogen atoms, the bound state ($\bar{p}e^+$), can be created by circulating the beam of an antiproton storage ring through an internal gas target. An antiproton that passes through the Coulomb field of a nucleus of charge Z will create e^+e^- pairs, and antihydrogen will form when a positron is created in a bound rather than a continuum state about the antiproton. The cross section for this process is calculated to be $\sim 4Z^2$ pb for antiproton momenta above 6 GeV/c. The gas target of Fermilab Accumulator experiment E760 has already produced ~ 34 unobserved antihydrogen atoms, and a sample of ~ 760 is expected in 1995 from the successive experiment E835. No other source of antihydrogen exists. A simple method for detecting relativistic antihydrogen is proposed and method outlined of measuring the antihydrogen Lamb shift to $\sim 1\%$.

PACS number(s): 13.75.Cs, 11.30.Er, 36.10.−k

I. INTRODUCTION

Antihydrogen, the simplest atomic bound state of antimatter, $\bar{H} \equiv (e^+\bar{p})$, has never been observed. A long-sought goal of atomic physics is to produce sufficient numbers of antihydrogen atoms to confirm the *CPT* invariance of bound states in quantum electrodynamics, for example, by verifying the equivalence of the $2S_{1/2}-2P_{1/2}$ Lamb shifts of H and $\bar{H}$.

Many sources of antihydrogen have been proposed and are under development [1]. The processes to be used include the radiative capture of slow positrons with antiprotons, possibly stimulated by a laser, charge exchange in the collision of an antiproton with positronium, possibly pumped to a Rydberg state, and three-body recombination of positrons and antiprotons in a cold-trapped plasma. No antihydrogen has yet been made by any of these processes, yet curiously a working source already exists that uses the collision of relativistic antiprotons with ordinary atoms. An antiproton passing through the Coulomb field of a nucleus of charge Z will create electron-positron pairs; occasionally a positron will appear in a bound instead of a continuum state about the moving antiproton and form antihydrogen. The cross section for this capture process we calculate to be

$$\sigma(\bar{p}Z \to \bar{H}e^- Z) \sim 4Z^2 \text{ pb}$$

for antiproton momenta above ~ 6 GeV/c. Fermilab experiment E760 has studied $\bar{p}p$ annihilation in the Fermilab Accumulator (an antiproton storage ring) using an internal H_2 gas target; the luminosity integrated of 9 pb^{-1} corresponds to a sample of 34 (undetected) antihydrogen atoms. The successive experiment E835, scheduled to run in 1995, will integrate a sample of 200 pb^{-1} and will produce 760 antihydrogen atoms.

Evidently, $\bar{p}$-storage rings with internal gas targets can make small numbers of antihydrogen atoms. We focus hereafter on their detection at the Fermilab accumulator ring operating at a model momentum of 3 GeV/c, but the methods will apply to their detection at any $\bar{p}$ storage ring operating at this or any higher momentum. We find that each antihydrogen atom can be detected with essentially unit efficiency and zero background, using an apparatus compatible with the simultaneous operation of experiments such as E760 and E835 that study $\bar{p}p$ annihilation. With a sample of only $\sim 3\times 10^4$ atoms, it is possible to measure the antihydrogen Lamb shift to a precision of $\sim 1\%$, and thus probe for anomalous, *CPT*-violating interactions between the position and antiproton that would change the binding energy of either the $2s$ or $2p$ state by 2 parts in 10^8. As methods of cooling stored antiproton beams improve, it may be possible to increase the rate of antihydrogen production several orders of magnitude by using a high-Z target gas such as xenon to take advantage of the Z^2 dependence of the production cross section.

A close analogue to the $\bar{H}$ formation process examined here is electron capture in relativistic heavy-ion collisions $Z_1Z_2 \to (Z_1e^-)e^+Z_2$. This process has so large a cross section for changing the charge of a circulating beam that it caps the luminosity achievable at relativistic heavy-ion colliders (RHIC's) such as the BNL RHIC [2]. Other analogues may be found in particle physics; a number of features observed in the production of heavy quark hadrons in high-energy hadronic collisions, particularly at large momentum fractions, can be understood as the coalescence of a produced heavy quark with the spectator quarks in the hadrons in either the beam or the target [3].

II. CROSS-SECTION CALCULATION

The production process for antihydrogen studied in this paper is the exclusive two- to three-particle reaction

 ©1994 The American Physical Society

$\bar{p}p \to \bar{H}e^- p'$, shown in Fig. 1. The equivalent photon approximation [4], applied in the antiproton rest frame, relates the cross section for pair creation with capture to the $1s$ state, $\bar{p}Z \to \bar{H}(1s)e^- Z$, to the cross section for photon-induced capture using virtual photons, $\gamma^* \bar{p} \to e^- \bar{H}(1s)$. Consistent with this approximation, we assume the $\bar{p}$ and the $\bar{H}$ in these processes remain at rest in a common frame of reference, and in this frame neglect the electron and photon energies compared with the antiproton mass. We find

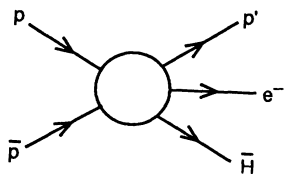

FIG. 1. The exclusive two- to three-particle reaction $\bar{p}p \to \bar{H}e^- p'$.

$$\sigma_{\bar{p}Z \to \bar{H}(1s)e^- Z} = \frac{Z^2\alpha}{\pi} \int_{2m/E}^{1} \frac{dx}{x} \int_0^{q_{\perp \max}^2} dq_\perp^2 \frac{q_\perp^2}{(q_\perp^2 + x^2M^2)^2} \left[\frac{1+(1-x)^2}{2} \right] \sigma_{\gamma^* \bar{p} \to \bar{H}(1s)e^-}(\omega, q^2) \ . \tag{1}$$

Here $x = \omega/E = \omega/(M\gamma)$ is the photon energy fraction evaluated in the antiproton rest frame, $q_\perp$ is the photon's transverse momentum, and M is the antiproton mass. At large photon virtuality $Q^2 = -q^2$, the photoabsorption cross section falls off as $(Q^2 + 4m_e^2)^{-1}$, so the transverse momentum $q_\perp$ in the integrand is typically of order $2m_e$. The upper limit of integration $q_{\perp \max}$ has the same order of magnitude as the photon energy ω because the photon tends to have $q^2 \approx 0$.

The contributions where q^2 is small dominate the integral, so we can set $q^2 \approx 0$ and substitute the cross section for real instead of virtual photons. Performing the integration over $q_\perp^2$, we find that the total cross-section factors

$$\sigma_{\bar{p}Z \to \bar{H}(1s)e^- Z}(\gamma) = Z^2 F(\gamma) \frac{\alpha}{\pi} \bar{\sigma} \ , \tag{2}$$

where

$$F(\gamma) = \ln(\gamma^2 + 1) - \frac{\gamma^2}{\gamma^2 + 1} \tag{3}$$

contains the dependence on the relative velocity of the antiproton and the nucleus, where γ is the Lorentz factor $\gamma = (1-\beta^2)^{-1/2}$, and where

$$\bar{\sigma} = \int_{2m_e}^{E} \frac{d\omega}{\omega} \sigma_{\gamma \bar{p} \to \bar{H}(1s)e^-}(\omega) \tag{4}$$

is a constant.

Crossing symmetry relates the matrix elements for photon-induced capture and for photoionization: the sum over initial and final spins of the squares of the matrix elements for the reactions $\gamma \bar{p} \to e^- \bar{H}(1s)$ and $\gamma \bar{H}(1s) \to e^- \bar{p}$ become equal if they are written in terms of the Mandelstam variables s, t, and u, and if the variables s and u in one element are exchanged. The squares of the matrix elements when the final spins are summed but the initial spins are averaged, $|M|^2$, are likewise related, except that a factor of 2 is introduced:

$$|M|^2_{\text{capture}}(s,t,u) = 2|M|^2_{\text{photo}}(u,t,s) \ . \tag{5}$$

The matrix element for photoionization in the $\bar{p}$ rest frame is given by [4]

$$|M|^2_{\text{photo}} = \frac{(32\pi)^2\alpha^6 m^4 M^2}{(\mathbf{k}-\mathbf{p})^4} \left[\frac{a^2p^2m}{\epsilon+m} + a(\mathbf{k}\cdot\mathbf{p} - p^2) \left[\frac{1}{k^2-p^2} + \frac{1}{(\mathbf{k}-\mathbf{p})^2} \right] + \frac{\epsilon+m}{4m}(\mathbf{k}-\mathbf{p})^2 \left[\frac{1}{k^2-p^2} + \frac{1}{(\mathbf{k}-\mathbf{p})^2} \right]^2 \right.$$
$$\left. - \frac{\epsilon+m}{2m} \frac{k^2p^2 - (\mathbf{k}\cdot\mathbf{p})^2}{(k^2-p^2)(\mathbf{k}-\mathbf{p})^2k^2} + a\frac{k^2p^2-(\mathbf{k}\cdot\mathbf{p})^2}{(\mathbf{k}-\mathbf{p})^2k^2} \right] , \tag{6}$$

where the quantity a is given by

$$a = \frac{1}{(\mathbf{k}-\mathbf{p})^2} + \frac{\epsilon}{m(k^2-p^2)} \ , \tag{7}$$

and where $\mathbf{p}$ and $\mathbf{k}$ are, respectively, the momentum vectors of the outgoing electron and incoming photon, and $\epsilon = \sqrt{|\mathbf{p}|^2 + m^2}$ is the electron energy. We define also $p = |\mathbf{p}|$ and $k = |\mathbf{k}| = \omega$. We can write the photoionization matrix element in terms of the Mandelstam variables, which in the $\bar{p}$ rest frame are equal to

$$\begin{aligned} s &= M^2 + 2M\omega \ , \\ t &= m^2 - 2\omega\epsilon + 2\mathbf{k}\cdot\mathbf{p} \ , \\ u &= M^2 - 2\epsilon M + m^2 \ . \end{aligned} \tag{8}$$

After interchanging s and u, and using Eq. (5), we get the capture matrix element. The total cross section for photon-induced capture is

$$\sigma_{\gamma \bar{p} \to e^- \bar{H}(1s)}(\omega) = \frac{p}{64\pi^2\omega M^2} \int |M|^2_{\text{capture}} d\Omega_e \ . \tag{9}$$

Integrating Eqs. (4) and (9) numerically yields $(\alpha/\pi)\bar{\sigma} = 1.42$ pb. Using Eq. (2), we get the cross section for $\bar{p}Z \to \bar{H}(1s)e^- Z$ as a function of the antiproton momentum; as shown in Table I, it is approximately $4Z^2$ pb for momenta above ~ 6 GeV/c. Capture into states of higher principal quantum number will increase the total cross section for capture by ~ 10–20%.

TABLE I. Cross section (σ) for the production of antihydrogen in the 1s state by antiprotons incident on a proton target, as a function of the Lorentz factor $\gamma = E_{\bar{p}}^{\rm lab}/M$ of the antiproton. For other targets, the cross section for $\bar{p}Z \to \bar{H}Ze^-$ scales as Z^2.

γ	σ (pbarn)
3	2.0
6	3.8
10	5.2
50	9.7
100	11.7
200	13.6

Calculations of similar cross sections have been reviewed by Eichler [5], and give

$$\sigma(\bar{p}p \to \bar{H}pe^-) = 2.7 \ln(\gamma) \text{ pb} ,$$

which is very close to our asymptotic result $\sigma = 2.8 \ln(\gamma)$ pb. Rhoades-Brown and co-workers [6] give a value of $\sigma = 2.8$ pb for the same cross section at $\gamma = 6$, which is not far from our result of $\sigma = 3.8$ pb. Finally, Becker [7] computes the cross section for two different momenta; the ratio of the cross sections agrees remarkably well with that predicted by Eq. (3), though his cross sections are lower than ours by a factor of 2.8.

To get the cross section for electron capture in heavy-ion collisions, $Z_1 Z_2 \to (Z_1 e^-) Z_2 e^+$, where the electron is captured in the 1s state of the nucleus Z_1, we need only set $Z = Z_2$ and multiply our cross section by

$$Z_1^5 \frac{2\pi\alpha Z_1}{e^{2\pi\alpha Z_1} - 1} . \tag{10}$$

This factor accounts for the increase in the square of the atomic wave function at the origin, and scales as Z_1^5 for $\alpha Z_1 \ll 1$.

An important issue for a practical experiment is the characteristic transverse momentum scale of the emerging antihydrogen atoms. Since the cross section is controlled by the underlying e^+e^- pair production process, the outgoing electron will be produced with a characteristic transverse momentum scale $p_\perp^e \sim m_e$. The capture process that forms the antihydrogen is a soft process that occurs at low relative positron-antiproton velocity; thus, one might guess that the $\bar{H}$ will be dominantly produced at transverse momenta $k_\perp$ of the order of the Bohr momentum scale αm_e. In such a case, the outgoing proton would almost entirely balance the electron's transverse momentum. In fact, this intuition is not correct: we shall show that the antiatoms emerge with transverse momenta of order m_e.

The physics can be understood most easily by working in the $\bar{p}$ rest frame. A typical time-ordered diagram that contributes to the capture reaction is shown in Fig. 2. In the heavy mass limit, we only need to consider the exchange of Coulomb photons with the target $\bar{p}$. The $\bar{H}$ wave function is a strongly peaked function of the relative momentum

$$\mathbf{v} = \mathbf{l} - (M_{\bar{p}}/M_{\bar{H}})\mathbf{k} \sim \mathbf{l} - \mathbf{k} .$$

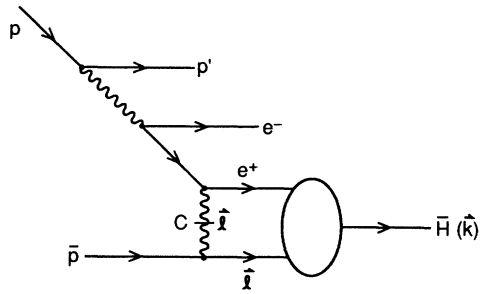

FIG. 2. A typical time-ordered diagram that shows, in the heavy-mass limit $M \gg m$, the exchange of Coulomb photons with the target $\bar{p}$.

Since

$$\mathbf{k}^2 \sim \mathbf{l}^2 \sim m_e^2 \gg \mathbf{v}^2 \sim (\alpha m_e)^2 ,$$

the three-momentum loop integration over the bound-state wave function factors out:

$$\int d^3\mathbf{v} \frac{1}{l^2}\psi(\mathbf{v}) \sim \frac{1}{l^2}\int d^3\mathbf{v}\,\psi(\mathbf{v}) \sim \frac{1}{l^2}\psi(\mathbf{r}=0) . \tag{11}$$

Thus the $\bar{H}$ recoils the transverse momenta $k_\perp \sim l_\perp \sim m_e$, and distribution of $\bar{H}$ momenta does not differ significantly from that of the $\bar{p}$ in the no-capture reaction; the capture process can be considered a final-state effect that does not modify the kinematics of underlying pair production reaction $\bar{p}p \to \bar{p}\,'e^+e^-p'$. The rate of capture is set by the antihydrogen's wave function at the origin.

This analysis also justifies the use of the equivalent photon approximation used in Eq. (1), since the fact that the photon attached to the proton is virtual does not significantly modify the kinematics of the capture reaction.

III. PROPERTIES OF A 3 GeV/c $\bar{H}$ BEAM

The momentum transferred to the antiproton in the process $\bar{p}Z \to \bar{H}e^-Z$ is small, the order of $mc \sim 5\times10^{-4}$ GeV/c. The momentum and position vectors of an antihydrogen atom are therefore the same as those of the antiproton from which it forms; a monoenergetic, small-divergence bunch of antiprotons exits a cloud of gas overlapped by an equivalent bunch of antihydrogen atoms. The distribution in transverse momentum of a stochastically cooled antiproton beam is narrow, so an antihydrogen beam has a small angular divergence. Experiment E760, when operated at an antiproton momentum of $\gtrsim 3$ GeV/c, achieved a beam in its gas target whose standard deviation in height and in angle were, respectively, $\sigma_y = 0.14$ cm and $\sigma_{\theta y} = 2.4\times10^{-4}$ rad. After a 15 m flight, sufficient [8] for the neutral antihydrogen beam to pass through the first dipole magnet of the accumulator ring and escape, the beam height is $\sigma_y \approx 0.39$ cm, small enough for the beam to stay within the beam pipe whose vertical half-aperture is 2.3 cm [8]. Even 55 m from the gas target the beam height has a σ_y of only 1.2 cm; the antihydrogen appears as an isolated, small-emittance beam. An experiment to detect this beam can be set up outside the storage ring where it will not interfere with

the simultaneous running of $\bar{p}p$ annihilation experiments such as E835, and where the flux of spurious particles originating in the gas jet will be attenuated by the distance from the target gas.

The antihydrogen atoms escape the gas intact. A fast antihydrogen atom when it collides with an ordinary molecule will separate into a free positron and antiproton. Data for the separation cross section for monatomic hydrogen beams at 0.29 GeV/c [9], extrapolated [10] to a beam momentum of 3 GeV/c, yield values of 2.5×10^{-20} cm^2, 2.7×10^{-19} cm^2, and 3.3×10^{-19} cm^2 per H_2, N_2, and CH_4 target gas molecule, respectively. The probability that an antihydrogen atom will separate before leaving the E835 H_2 gas target, which has a column density of 10^{14} molecules/cm^2, is less than 10^{-4} even if the target consists [11] entirely of microdroplets of $\sim10^5$–10^6 molecules per droplet. At the accumulator this target provides a luminosity for $\bar{p}p$ annihilation of 10^{31} cm^{-2}s^{-1}; assuming a 3.5 pb production cross section, separation in the gas target will be unimportant unless its density is raised until the antihydrogen rate is ~0.4 s^{-1}. Antihydrogen can be transported through a rough vacuum; 10 m travel through even 1 mTorr of nitrogen gas will separate only $\sim1\%$ of the antihydrogen beam.

Antihydrogen easily survives its escape through the dipole fields of the accumulator ring. It forms mostly in atomic s states populated with a probability expected to diminish with principal quantum number n roughly as $1/n^3$. A laboratory magnetic field generates in the antihydrogen rest frame a large electric field in which a state may ionize. We ignore the effect of the remaining magnetic field on the ionization rate; in a uniform electric field the rate of ionization of a state with parabolic quantum numbers [12] n, n_2, and m is [13]

$$R\sim\frac{1}{n^3 n_2!(n_2+|m|)!}\left[\frac{n^3|\mathbf{E}|}{4}\right]^{-2n_2-|m|-1}\times\exp[3(n-2n_2-m)-2/(3n^3|\mathbf{E}|)]\frac{\alpha^2mc^2}{\hbar}\ , \quad (12)$$

where $|\mathbf{E}|$ is the applied electric field in units of $e^2/a_0=5.142\times10^9$ V/cm, and where a_0 is the Bohr radius. To escape the atom, a positron must tunnel out of a Coulomb potential well, so that the ionization rate depends drastically on the well depth, and so on the principal quantum number n. For the maximum accumulator momentum of 8.83 GeV/c and dipole strength of 16.7 kG [8] the rest ionization rate of the 1s state is a negligible 4.3×10^{-13} s^{-1}, while the rate for the most stable of the $n=2$ states is $6.4\times10^{+14}$ s^{-1}. While the 2s state can therefore travel only a few microns in the field, the initial 2s population will nonetheless contribute to the flux of antihydrogen from the accumulator. A stray field of only ~1 G transforms into a large enough electric field to mix the 2s state completely with the nearly degenerate 2p state, and to induce an electric dipole transition to the 1s state with a rate of 3.2×10^8 s^{-1}. This is fast enough to transfer most atoms in the 2s state to the 1s before they can travel 15 m to the first bend magnet and can ionize.

Because the production cross section scales as Z^2, the flux of antihydrogen might be raised a factor of 3100 by replacing the hydrogen in the gas target with the same atomic density of xenon ($Z=56$). Backgrounds shrink and the yield goes up: the ratios of the numbers of nuclear events, scattered target electrons, and bremsstrahlung photons to the number of antihydrogen atoms made all diminish by roughly a factor of 100, and the antihydrogen yield per circulating antiproton increases from $\sim2\times10^{-10}$ to $\sim2\times10^{-8}$. However, the heating of the beam by multiple Coulomb scattering also scales as Z^2; if this heating now limits the luminosity achievable in active experiments on $\bar{p}p$ annihilation in hydrogen, then raising the rate of antihydrogen production by using a high-Z target will require improvements in beam cooling. The luminosity of experiment E835 is within a factor of 5–10 of being so limited [14], so only a factor of 5–10 increase in rate can presently be realized, and at the cost of changing the experiment from one operating parasitically to one requiring expensive dedicate running of the accumulator.

IV. DETECTION OF ANTIHYDROGEN AT 3 GeV/c

Fast antihydrogen separates into a pair of free particles with a probability greater than 0.99 in a mere membrane of polyethylene 400 μg cm^2 thick [15]. It therefore produces a pair of particles more readily than can anything else; the probability that a photon converts or that a hadron interacts in such a thin membrane are respectively only $\sim2.7\times10^{-5}$ and 6.6×10^{-7} [16]. Despite the initial Fermi momentum of the 1s state, the momentum transfer in the collision that frees the positron, and the subsequent large-angle and (multiple) small-angle scattering of the positron in the membrane, more than 99% of the positrons exit in a ±0.10-radian cone about the antiproton direction [17]. The longitudinal Fermi momentum of the 1s state, $\langle p_l^2\rangle^{1/2}=\sqrt{1/3}\alpha mc$, smears the nominal kinetic energy with which the positrons emerge from the membrane, $K=1.200$ MeV, by $\sigma_K=6.9$ keV; the positrons lose only 1.4 keV on average traversing the membrane [18]. The antiproton hardly scatters at all, and retains the tiny spread in transverse momentum the antiprotons have in the accumulator, $\delta p_t/p\sim2\times10^{-4}$.

An antihydrogen atom therefore generates in coincidence, from some point in a known, few-square-centimeter area of a membrane possibly tens of meters from the gas target, a positron and an antiproton with a common and tightly constrained velocity equal to the known velocity of the antiprotons circulating in the storage ring. So spectacular is this signature that the chief difficulty in designing an apparatus to detect antihydrogen is to choose which of many sufficient schemes is the simplest. The following scheme is the basis for a proposed experiment [19], Fermilab P862. An antihydrogen atom exits the accumulator ring and strikes a 400 μg cm^{-2} membrane, where it separates into a positron and an antiproton. Because the particles' magnetic rigidities differ by a factor of nearly 2000, the positron can be bent away and focused while hardly affecting the antiproton, so the particles can be directed into separated detectors. We describe how these detectors function for an antihydrogen momentum of 3 GeV/c; the apparatus works

equally well up to the maximum accumulator momentum of 8.8 GeV/c merely by scaling various magnetic fields.

A positron spectrometer a few meters in length, consisting in succession of a solenoid lens, a sector magnet, and a second solenoid lens, separates the positrons and focuses them onto a few-square-centimeter spot. A momentum resolution of a few percent matches the Fermi smear in the momentum of the positrons. The positrons stop in a scintillator ~ 1 cm thick whose total volume is only a few cubic centimeters. Light from the scintillator is guided into a single phototube; the rise and height of the output pulse give, respectively, a measure of the arrival time of the positron within 1 ns, and a measure of its kinetic energy to 20%. A 4π NaI detector surrounds the scintillator and intercepts the two 511 keV photons from the positron's annihilation; the detector also vetoes the passage of stray charged particles, which deposit far more energy than 511 keV. The collection efficiency of the spectrometer is 99%. Some 95% of the positrons come to rest in the scintillator and deposit their full energy; the 5% that backscatter nonetheless deposit enough energy to make a signal, and still come to rest and annihilate in the volume surrounded by NaI.

Tagging the antiproton is straightforward. Over a flight distance of 40 m, it passes through a pair of scintillator paddles that measure its velocity by time of flight, a sequence of multiwire proportional chambers (MWPC's) and bend magnets that measure its momentum to 0.2%, and a terminal Čerenkov threshold detector that provides a redundant velocity separation of antiprotons and other negative particles. The tiny beam spot, angular divergence, and unique and known velocity of the antiproton favor a differential-velocity Čerenkov detector [20], but for momenta as low as 3 GeV/c, it is difficult to generate enough light for such a device without using a Čerenkov medium so thick that antiprotons do not survive their passage.

A candidate antiproton is defined by hits in the MWPC's consistent with a 3 GeV/c antiproton that originates in the right few-square-centimeter area of the membrane, by the absence of a hit in the Čerenkov threshold detector, and by hits in the time-of-flight scintillators that are consistent with the passage of the particle of the right velocity. A candidate positron is defined by a hit in the positron scintillator with the right deposit of kinetic energy, coincident within a few nanoseconds with a hit in the surrounding NaI, consistent with the absorption or Compton scatter of two 511-keV photons. An antihydrogen candidate is defined as a subnanosecond coincidence between antiproton and positron candidates.

V. BACKGROUNDS

Despite the $\sim 10^{10}$ times higher cross section for $\bar{p}p$ annihilation than for antihydrogen production, the backgrounds from particles originating in the gas target will be zero. Here we consider only those processes which have such peculiar kinematics and large branching ratio as to mimic at least part of an antihydrogen signal, most importantly the antiproton, without requiring a failure of some part of the detector.

The only particle that can satisfy the momentum and velocity measurements made by the particle tracking, and by the time-of-flight and Čerenkov detectors, is an antiproton. Antiprotons lost from the ring are unimportant; few thread properly through the target and the wire chambers, and the passage of an antiproton through even an extra 2 cm of aluminum will slow the antiproton below the 0.2% momentum resolution of the particle tracking. The only plausible source of antiprotons is from antineutrons, made in the target by the charge-exchange reaction $\bar{p}p \rightarrow \bar{n}n$, that convert by a second charge-exchange reaction into an antiproton. The simplest possibility is for an antineutron generated in the gas target to pass undeflected through the accumulator's dipole magnet and convert in the first MWPC; the new antiproton fools the rest of the detectors in our antiproton beam line. Of all processes that make antiprotons, this one has the most dangerous combination of unfavorable kinematics and large relevant cross sections. The number of $\bar{n}$'s made in the gas target is large; both the neutral $\bar{n}$'s and the converted $\bar{p}$'s are thrown forward, the more easily to pass through the apparatus and the antiproton beam line; and the forward $\bar{p}$'s from this two-step process can have precisely the same velocity as the antiprotons circulating in the ring [21].

Nonetheless, the beam line will count fewer antiprotons from this process than it will count antiprotons from antihydrogen. The count rate is small principally because of the small solid angle subtended by the known small spots (of order 3 cm^2) that legitimate antiprotons make on both the first and last MWPC's, compared to the typical solid angle over which particles from charge exchange are distributed. At a model momentum of $p=3$ GeV/c, the cross section for $\bar{p}p \rightarrow n\bar{n}$ is 2.0 mbarn [22]; an integrated luminosity of 200 pb^{-1} will produce 4.0×10^{11} antineutrons. In charge exchange, the typical momentum transfer is the order of the pion mass, $\delta p \sim 135$ MeV/c, and so the outgoing antineutrons will be distributed over a solid angle that is the order of $\Delta\Omega \sim \pi(\delta p/p)^2 \sim 6.4\times 10^{-3}$ steradian. The thickest material in front of all the MWPC's is 0.3 cm of scintillator in the first time-of-flight detector. Reconstruction of the antiproton track limits the active area on this scintillator to roughly 3 cm^2; the solid angle of this spot as seen from the gas target, 20 m away, is only 7.5×10^{-7} steradian, and the probability any antineutron from charge exchange hits the spot is only 1.2×10^{-4}. The probability of a hadronic interaction in the scintillator is only 3.8×10^{-3}; if an antineutron interacts, it will generate an antiproton with a probability equal to the ratio of the cross section for charge exchange to the total cross section, which for a proton target is equal [22] to

$$2.0 \text{ mbarn}/79.9 \text{ mbarn} = 2.5\times 10^{-2} .$$

Any antiproton made must now pass through the antiproton beam line and strike a 3 cm^2 spot on the last MWPC, at least 20 m away; because of the momentum transfer in charge exchange, the probability it will do so is again only 1.2×10^{-4}. Collecting all the factors, the number of antiprotons from this process indistinguish-

able from the 760 antiprotons we expect from the separation of antihydrogen is at most

$$(4.0\times10^{11})(1.2\times10^{-4})(3.8\times10^{-3})(2.5\times10^{-2})\times(1.2\times10^{-4})=0.5\ .$$

This order-of-magnitude argument is quite crude, but sufficient to show that the rate of such false antiprotons, occurring in coincidence with a positron candidate, is certainly negligible.

The charge exchange of antineutrons anywhere else in harmless. The path of a candidate antiproton, determined by hits in the MWPC's, extrapolates back through the dipole magnet of a storage ring to intercept the vertical inner wall of the ring at a finite angle. At the accumulator, an antiproton from charge-exchange must emerge at a full 5° with respect to the direction of the incident antineutron. The drop in momentum is fifteen times the 0.2% resolution we expect from tracking the antiproton. Furthermore, for an integrated luminosity of 200 pb^{-1}, we estimate that only six antiprotons so generated in the beam pipe, whether they have the right momentum and velocity or not, will even strike the required 3 cm^2 area in our last MWPC.

The kinematics of an antineutron's ordinary β decay, $\bar{n}\rightarrow\bar{p}e^{+}\nu$, are also unfavorable because the decay produces not only a 3 GeV/c antiproton but also a positron whose range of laboratory kinetic energy overlaps 1.200 MeV; fortunately, its slow decay rate $\sim10^{-3}$ s^{-1} prevents a significant fraction from decaying within our apparatus.

VI. OTHER EXPERIMENTS WITH RELATIVISTIC ANTIHYDROGEN

To test *CPT* invariance it is best to study hydrogen and antihydrogen in the same apparatus. The polarity of the magnets in the Fermilab accumulator can be reversed and protons circulated; as the protons pass through the target gas, they pick up atomic electrons and make a neutral hydrogen beam that has the same optics as the antiproton beam. For protons above 3 GeV/c, the dominant process [23] is one in which an essentially free electron in the target falls into the 1s state and a photon carries off the binding energy. The cross section [24] per target electron is $\gtrsim1.7$ nb, so for equal circulating currents through a hydrogen gas target the hydrogen beam will have ~430 times the intensity of the antihydrogen beam.

Two experiments seem practical with meager samples respectively of order 10^3 and 3×10^4 antihydrogen atoms. The first is a measurement of the rate of field ionization of the $n=2$ states in an electric field provided by the Lorentz transform of a laboratory magnetic field. Roughly 10% of a 3 GeV/c beam of antihydrogen in the 1s state can be excited into states with $n=2$ by passing it through a thin membrane. If the membrane sits in a 20 kG transverse magnetic field, Eq. (12) shows that the states with $n>2$ will ionize instantly, that the states with $n=2$ will ionize with $1/e$ decay lengths of order 10 cm, and that the 1s state will not ionize at all. The distance a state with $n=2$ flies before ionizing is marked by the deflection of the freed antiproton by the magnetic field by an amount between the zero deflection of the surviving 1s component of the beam and the large deflection of the antihydrogen that ionizes instantly or separates in the membrane. Ten centimeters of flight before ionization changes the deflection of the antiproton seen 3 m away by 6.7 cm, many times the antiproton spot size of $\lesssim1$ cm; and changes the antiprotons angle by 22 mrad, many times both its original angular divergence of 0.2 mrad and the resolution of 0.1 mrad that can be provided by a pair of MWPC's 10 m apart with 1 mm resolution. The distance a state flies is also marked by the freed positron, whose orbit radius is only 2 mm in the transverse field, and which can be directed along the field lines into some sort of position-sensitive detector. The positron and antiproton have of course their usual known common velocity. A flux of a few thousand $\bar{H}$'s may be sufficient to measure the three distinct field ionization rates of the $n=2$ states to $\sim10\%$. Because ionization is a tunneling process, its rate is surprisingly sensitive to details of the antihydrogen wave function; a 10% shift would require, for example, a change in $\langle r\rangle$ for the $n=2$ states of only 0.24%.

Evidently ionization in a magnetic field can be used to count efficiently states with $n=2$, without counting states of different principal quantum number. No other method is available; the Accumulator runs with long antiproton bunches, and no laser has sufficient continuous power to photoionize efficiently the relativistic antihydrogen beam. By driving the 1000 MHz $2s-2p$ transition and monitoring the surviving 2s population as a function of frequency, the frequency of the antihydrogen Lamb shift can be measured. The $1/e$ decay length of the 2p states is 1.4 m at 3 GeV/c, and so a few meters from an excitation membrane only the 2s population will survive. The Doppler-shifted transition can be driven by chasing the beam with 6.1 GHz radiation aimed down a waveguide that is roughly 10 m long, and roughly 10 cm^2 in cross section; this guide may also serve as a beam pipe. The $2s-2p$ resonance has a quality factor of only ten because of the width of the 2p state, and so the Doppler broadening of the transition (or a misalignment of the axes of the beam and the guide) will not put the transition out of resonance. Because the $2s-2p$ transition is electric dipole in character and has a large matrix element, modest laboratory powers of roughly 10 W/cm^2 suffice [25] to mix the 2s state completely with the 2p and make the 2s state decay with a $1/e$ distance of 2.8 m. To prevent Stark mixing of the 2s and 2p states, transverse magnetic fields must be less than 0.1 G from the excitation membrane down the guide's length, until the sharp rise of the transverse magnetic field that is used to ionize and count the $n=2$ states. If the rise occurs over less than the fully mixed 2s decay length of 2.8 m, little of the 2s state will decay to the 1s instead of ionize. A sample of a 300 antihydrogen atoms in the 2s state would suffice to see a dip in the transmitted 2s population as a function of drive frequency, find its center to within 10% of its width, and so measure the antihydrogen Lamb shift to $\sim1\%$. A total of 3×10^4 antihydrogen atoms is enough to provide such a sample if a membrane yields as expected [26] 0.01 2s states per incident 1s. The experiment would be sensitive to a differential shift of the 2s and 2p states of hydro-

gen and antihydrogen equal to a fraction $\sim 2\times 10^{-8}$ of the states binding energy, and would test the *CPT* symmetry of the $e^+\bar{p}$ interaction at momentum scales characteristic of atomic binding, 10 eV/c.

ACKNOWLEDGMENTS

The authors gratefully acknowledge contributions to the design of the experiments made by A. Belkacem, D. C. Christian, H. Gould, M. Peskin, M. Mandelkern, R. H. Miller, G. Smith, and the members of the 1992 Fermilab Physics Advisory Committee. This work was supported in part by Department of Energy under Contract No. DE-AC03-76SF00515 (SLAC) and in part by Fondo Nacional de Investigación Científica y Tecnológica, Chile.

[1] Hyperfine Interact. **44** (1988); **76** (1993).

[2] RHIC Conceptual Design Report No. BNL 52195 (unpublished), Table IV.3-10 and pp. 118–120; also see Report No. BNL 52247 UC-414 (High Energy Physics-DOE/OSTI-4500-R75), Proceedings of the Workshop "Can RHIC be used to test QED?" edited by M. Fatyga, R. J. Rhoades-Brown, and M. J. Tannenbaum, April 20–21, 1990 (unpublished).

[3] For example, see S. J. Brodsky, J. F. Gunion, and D. E. Soper, Phys. Rev. D **36**, 2710 (1987); S. J. Brodsky and A. H. Mueller, Phys. Lett. B **206**, 685 (1988); R. Vogt, S. J. Brodsky, and P. Hoyer, Nucl. Phys. **B360**, 67 (1991); **B383**, 643 (1992).

[4] V. B. Berestetskii, E. M. Lifshitz, and L. P. Pitaevskii, *Relativistic Quantum Theory, Part 1,* 2nd ed. (Pergamon, New York, 1979), p. 212 [a missing factor of 2 has here been restored to their formulas; see, for example, W. Heitler, *The Quantum Theory of Radiation,* 3rd ed. (Oxford, New York, 1954), p. 209], and p. 438.

[5] J. Eichler, Phys. Rep. **193**, 165 (1990).

[6] M. J. Rhoades-Brown (private communication). A value of 3.1 pb for $\gamma=6$ can be extracted using from the cross section for a charge-changing collision of bare gold nuclei reported in M. J. Rhoades-Brown, C. Bottcher, and M. R. Strayer, Phys. Rev. A **40**, 2831 (1989); A. J. Baltz, M. J. Rhoades-Brown, and J. Weneser, *ibid.* **44**, 5569 (1991): the cross section should be divided by a factor of $Z^{6.6}$, and again by a factor of 2 to adjust for the possibility an electron is captured by either gold nucleus [M. J. Rhoades-Brown (private communication)].

[7] U. Becker, J. Phys. B **20**, 6563 (1987).

[8] Design Report, Tevatron 1 Project, September 1984.

[9] E. Acerbi, C. Birattari, B. Candoni, M. Castiglioni, D. Cutrupi, and C. Succi, Lett. Nuovo Cimento **10**, 598 (1974).

[10] In the Born approximation, where $Z\alpha/\beta \ll 1$ where Z is the target nuclear charge and β the velocity of the hydrogen atom, the cross section for stripping on a neutral atom varies with beam velocity merely as a constant times $1/\beta^2$. G. H. Gillespie and M. Inokuti, Phys. Rev. A **22**, 2430 (1980).

[11] M. Macri, in *Proceedings of the 1983 CERN 1st Accelerator School: Antiprotons for Colliding Beam Facilities,* Geneva, Switzerland, 1983, edited by P. Bryant and S. Newman (European Organization for Nuclear Research, Geneva, 1984).

[12] H. A. Bethe and E. E. Salpeter, *Quantum Mechanics of One- and Two-electron Atoms* (Academic, New York, 1957).

[13] T. Yamabe, A. Tachibana, and H. J. Silverstone, Phys. Rev. A **16**, 877 (1977), Eq. (125). This gives the asymptotic behavior of the ionization rate in the limit of small field $|\mathbf{E}|$; see also R. Haydock and D. R. Kingham, J. Phys. B **14**, 385 (1981).

[14] E835 Collaboration (private communication).

[15] The stripping cross section for monatomic hydrogen at 200 MeV on a carbon target has been measured to be $6(1)\times 10^{-19}$ cm^2 in R. C. Webber and C. Hojvat, IEEE Trans. Nucl. Sci. **NS-26**, 4012 (1979).

[16] Values of 14.70 g cm^{-2} and 60.2 g cm^{-2} for the radiation length and nuclear collision length in carbon are taken from the Particle Data Group, K. Hikasa *et al.*, Phys. Rev. D **45**, S1 (1992).

[17] A scatter through >0.10 radian requires a transfer of transverse momentum much greater than the (transverse) Fermi momentum of the 1s state, $\langle p_t^2\rangle^{1/2}=\sqrt{2/3}\alpha mc$, so that the probability for such a scatter may be calculated using the formula for simple Rutherford scattering; the probability is $\sim 8\times 10^{-3}$ for a 400 μg/cm^2 carbon target. This angle is safely more than three times the standard deviation of the approximately Gaussian distribution from small-angle multiple scattering.

[18] The dE/dx of a 1.20 MeV electron in carbon, which we use to estimate that of a positron, is 3.8 MeV cm^2 g^{-1}. See L. Pages, E. Bertel, H. Joffre, and L. Sklavenitis, At. Data **4**, 1 (1972).

[19] C. T. Munger, M. Mandelkern, J. Schultz, G. Zioulas, T. A. Armstrong, M. A. Hasan, R. A. Lewis, G. A. Smith, and D. Christian, Proposal for the Detection of Relativistic Antihydrogen Atoms Produced by Pair Production with Positron Capture, Fermilab Proposal P862, 1992 (unpublished).

[20] J. Litt and R. Meunier, Annu. Rev. Nucl. Sci. **23**, 1973; P. Duteil, L. Gilly, R. Meunier, J. P. Stoot, and M. Spighel, Rev. Sci. Instrum. **35**, 1523 (1964).

[21] The fractional drop in the momentum of the forward $\bar{p}$'s due to the neutron-proton mass difference is $\delta p/p=-1.4\times 10^{-3}$, which is comparable to but smaller than the resolution in momentum provided by tracking.

[22] A. Baldini, V. Flaminio, W. G. Moorhead, and D. R. O. Morrison, *Landolt-Börnstein Numerical Data and Functional Relationships in Science and Technology: Total Cross-Sections for Reactions of High Energy Particles* (Springer-Verlag, Berlin, 1988), Vol. 12b.

[23] R. Shakeshaft and L. Spruch, Rev. Mod. Phys. **51**, 369 (1979).

[24] The cross section for radiative capture of a free electron with Lorentz factor γ onto a charge Z is

$$\sigma_{rc}=4\pi\alpha^4 Z^5\left[\frac{e^2}{mc^2}\right]^2(\gamma-1)^{-5/2}(\gamma+1)^{+1/2}$$

$$\times\left[\frac{4}{3}+\frac{\gamma(\gamma-2)}{\gamma+1}\left[1-\frac{1}{2^\gamma(\gamma^2-1)}\ln\frac{\gamma+(\gamma^2+1)}{\gamma-(\gamma^2-1)}\right]\right].$$

This formula is adapted from G. Raisbeck and F. Yiou,

Phys. Rev. A **4**, 1958 (1971), after correcting an error these authors made transcribing the relativistic matrix element. See, for example, Heitler, *The Quantum Theory of Radiation* (Oxford, New York, 1954), Eq. V.22.45, and the original reference, F. Sauter, Ann. Phys. **9**, 454 (1931), Eq. 39.

[25] W. E. Lamb, Jr. and R. C. Retherford, Phys. Rev. **60**, 817 (1941).

[26] Coulomb collisions can excite the 1*s* state to the 2*s* and ionize both the 1*s* and the 2*s*. The cross sections for an unscreened nuclear charge may be found by amalgamating the work H. S. Massey, *The Theory of Atomic Collisions* (Clarendon, England, 1987); M. K. Prasad, Acta Phys. Pol. B **10**, 635 (1979); the maximum yield so predicted is 0.8%. However, a yeild of ~10% has been reported from the use of a 1000-Å Formvar membrane to excite a 65 MeV hydrogen beam; see V. V. Parkhomchuk, in *Antimatter '87: Production and Investigation of Atomic Antimatter* [1], p. 315.